THE JOURNAL OF PHYSICAL CHEMISTRY A LETTERS

**2009,** *113,* 6552–6554
Published on Web 05/26/2009

# Effect of the Dynamical Disorder on the Second-Order Nonlinear Optical Responses of Helicity-Encoded Polymer Strands

**Raphaël Méreau,[⊥,‡] Frédéric Castet,*[,⊥] Edith Botek,[†,#] and Benoît Champagne*[,†]**

*Institut des Sciences Moléculaires (ISM), UMR 5255 CNRS, Université de Bordeaux, Cours de la Libération 351, F-33405 Talence CEDEX, France, and Laboratoire de Chimie Théorique Appliquée, Facultés Universitaires Notre-Dame de la Paix (FUNDP), rue de Bruxelles 61, B-5000 Namur, Belgium*

*Received: May 12, 2009*

By combining classical samplings with quantum chemistry semiempirical time-dependent Hartree−Fock calculations, the high impact of dynamic fluctuations on the NLO properties of helical strands has been evidenced. In particular, these fluctuations are responsible for relative variations of ∼20% in the hyper-Rayleigh responses in both pyridine−pyrimidine (py−pym) and hydrazone−pyrimidine (hy−pym) strands. Then, dynamical disorder has an even more important impact on the electric-field-induced second harmonic generation responses, whose variations can reach 2 (py−pym) or 5 (hy−pym) times their mean value. This work also highlights the relationships between the unit cell nature and helical conformation of foldamers and their second-order NLO responses. In particular, the octupolar symmetry of the hyper-Rayleigh depolarization ratios is related to the helix periodicity of three unit cells per turn in both compounds.

For more than 30 years, the second-order nonlinear optical (NLO) properties of organic compounds, the first hyperpolarizabilities ($\beta$), have been actively studied both theoretically and experimentally[1] due to their large amplitude associated with short response times and the feasibility of molecular design. It has been recognized that enhanced $\beta$ values require (i) optimizing the conjugation length,[2] (ii) choosing appropriate substituents with specific donor (D) and acceptor (A) strengths,[3] (iii) modeling the shape and dimensionality of the $\pi$-electron network,[4] as well as (iv) tuning the charge.[5] Evidence was also given that vibrational (nuclear relaxation) components to $\beta$ can become important for some NLO processes,[3b,6] whereas recent works using Thomas−Kuhn sum rules to derive fundamental physical limits to molecular $\beta$ values[7] demonstrated, though these limits are still subject to discussion,[8] that there is still plenty of room to derive new systems with larger second-order NLO susceptibilities. Helical (chiral) structures are among the most intriguing systems to exhibit large second-order NLO responses. Their symmetry impacts the $\beta$ tensor. Then, helices present the advantage of providing a way for positioning peripheral substituents in a well-defined spatial arrangement, a condition for achieving substantial macroscopic second-order NLO responses. In addition to controlling the conformation and therefore the properties and functions, designing such supramolecular architectures with specific combinations of intramolecular and noncovalent intermolecular patterns can lead to the preparation of systems with targeted rigidity, tuning the transitions between helical and linear strands.[9,10] These dynamical functional systems are, for instance, employed to mimic biopolymers in order to understand their biological functions.

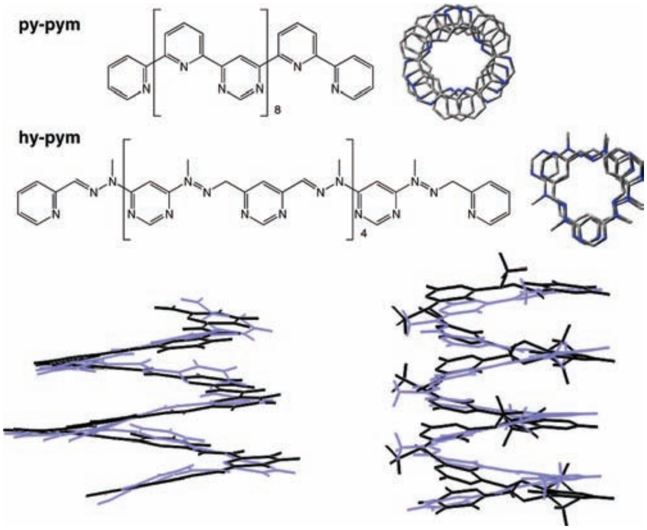

**Figure 1.** Top: Structure of pyridine−pyrimidine (py−pym) and hydrazone−pyrimidine (hy−pym) strands and top view showing the quasi $C_3$ symmetry. Bottom: Superimposition of the crystal structure (blue, ref 10) with the MMFF94 optimized structures of py−pym (left) and hy−pym (right).

We show here, on two representative helical systems of similar size prepared by Lehn and co-workers (Figure 1 (top)),[10] that the dynamical disorder strongly impacts the NLO properties.

These effects are investigated by combining classical Molecular Dynamics (MD) and quantum chemistry (QC) calculations. MD simulations were carried out in the canonical ensemble at room temperature, for 1 ns with time steps of 0.5 fs. The MMFF94 force field[11] was employed because it closely

---

* To whom correspondence should be addressed. E-mail: f.castet@ism.u-bordeaux1.fr (F.C.); benoit.champagne@fundp.ac.be (B.C.).

[⊥] Université de Bordeaux.

[†] FUNDP.

[‡] E-mail: r.mereau@ism.u-bordeaux1.fr.

[#] Email: edith.botek@fundp.ac.be.

10.1021/jp904418r CCC: $40.75

reproduces the structures of the helical strands, as determined from X-ray diffraction (Figure 1 (bottom) and ref 12). Every 2.5 ps, the geometrical structure was grasped, and the corresponding second harmonic generation $\beta(-2\omega;\omega,\omega)$ tensor was calculated for a wavelength of 1064 nm at the time-dependent Hartree–Fock (TDHF) level of approximation[13] with the semiempirical AM1 Hamiltonian.[14] A similar MMFF94//TDHF/AM1 computational scheme was recently used to evaluate the first hyperpolarizability of flexible epoxy oligomers including paranitroaniline chromophores.[15] Although it does not include explicitly electron correlation effects, it was substantiated in a series of works that the TDHF/AM1 approach is a good compromise between the quality of the results and the sparing of the computational resources for the calculation of the NLO responses of medium- and large-size systems.[16] Hyper-Rayleigh scattering (HRS) and electric-field-induced second harmonic generation (EFISHG) responses are analyzed because these are usual techniques to probe $\beta$.[17] In the case of plane-polarized incident light and observation made perpendicular to the propagation plane without polarization analysis of the scattered beam, the second-order NLO response that can be extracted from HRS data reads

$$\beta_{\mathrm{HRS}}(-2\omega;\omega,\omega) = \sqrt{\{\langle\beta_{ZZZ}^2\rangle + \langle\beta_{XZZ}^2\rangle\}}$$

while the associated depolarization ratio (DR) is given by

$$\mathrm{DR} = \frac{\langle\beta_{ZZZ}^2\rangle}{\langle\beta_{XZZ}^2\rangle}$$

This last quantity gives information on the geometry of the part of the molecule responsible for the NLO response (for an ideal D/A one-dimensional system, DR = 5, for an octupolar molecule, DR = 1.5, whereas for a Λ-shape molecule, the amplitude of DR depends on the angle between the chromophore as well as on the D/A groups[18]). Full expressions of the orientational averages of the $\beta$ tensor are given in the Supporting Information (SI). The EFISHG measurements give information on the projection of the vector part of $\beta$ on the dipole moment vector

$$\beta_{||}(-2\omega;\omega,\omega) = \beta_{||} = \frac{3}{5}\sum_{\zeta}^{x,y,z}\frac{\mu_\zeta}{||\mu||}\sum_{\eta}^{x,y,z}(\beta_{\zeta\eta\eta} + \beta_{\eta\zeta\eta} + \beta_{\eta\eta\zeta}) = \frac{3}{5}\sum_{\zeta}^{x,y,z}\frac{\mu_\zeta\beta_\zeta}{||\mu||}$$

where $||\mu||$ is the norm of the dipole moment and $\mu_i$ and $\beta_i$ are the components of the $\mu$ and $\beta$ vectors. For both systems, it has been verified that the parameters used in MDs enable sampling of all conformations and therefore determination of average quantities (Figure 2). Calculations were done using the MacroModel[19] and MOPAC[20] packages.

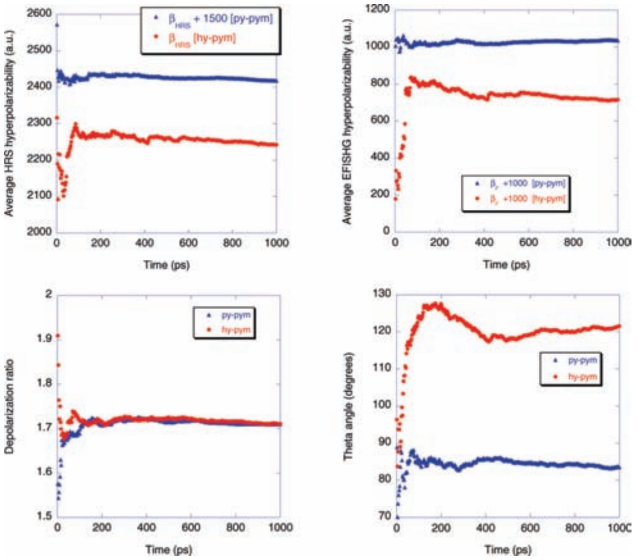

**Figure 2.** Evolution of the average values of HRS ($\beta_{\mathrm{HRS}}$ and the depolarization ratio) and EFISHG ($\beta$ and the angle between the $\mu$ and $\beta$ vectors) quantities as a function of the MD simulation time, demonstrating that they converge when considering a 1 ns dynamics with a 0.5 fs time step.

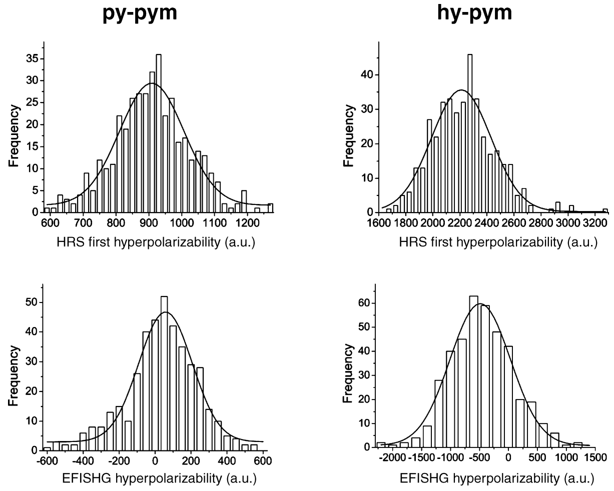

**Figure 3.** Distribution of the HRS (top) and EFISHG (bottom) $\beta$ values (in atomic units) along a MD simulation of 1 ns at 300 K in py–pym (left) and hy–pym (right) foldamers. A fit with a Gaussian distribution is done in each case.

The distributions of the $\beta$ values reported in Figure 3 show that the average $\beta_{\mathrm{HRS}}$ response of hy–pym is 150% larger than that for py–pym ($22 \times 10^2$ versus $9 \times 10^2$ au). Nevertheless, both structures present an average depolarization ratio of about 1.7 (Figures S11–S12, SI), characterizing octupolar-like NLO-phores.[21] The octupolar symmetry originates from the structure and assembly of the unit cells; three py–pym or hy–pym (Figure 1) units make slightly more than one helical turn so that both systems exhibit a quasi $C_3$ symmetry. This symmetry is also consistent with the fact that $\beta$ is dominated by its radial component and that the axial contribution is negligible.[12]

As also shown in Figure 3, the $\beta_{\mathrm{HRS}}$ distribution of the hy–pym presents a larger broadening than the one of py–pym (with respective standard deviations $\sigma$ of $2 \times 10^2$ and $4 \times 10^2$ au), owing to the larger flexibility of the monomer unit. The Gaussian distributions of the geometrical parameters, given in SI, show that the dihedral angles of both structures fluctuate in the range of 10–20°, while bond lengths display variations between 0.04 and 0.07 Å. As a key structural feature at the origin of important changes in the first hyperpolarizability of push–pull organic chromophores, the distributions in the bond length alternation[22] (BLA) for relevant bonds along the conjugated bridge in the hy–pym structure have also been analyzed (Figures S7–S8, SI). The large average BLA values (0.26 Å) indicate that the nature of the chemical bonds, as defined in the Lewis picture, is kept unchanged along the dynamics.

The EFISHG responses of the two structures are very different (Figure 3), with an almost negligible average value for the

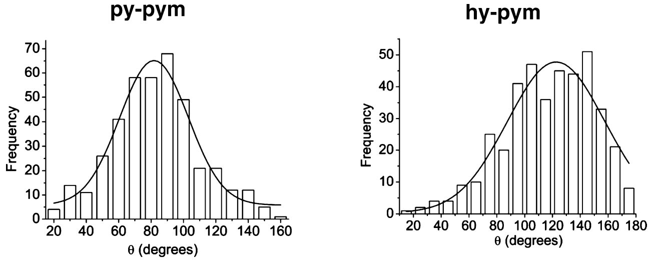

**Figure 4.** Distribution of the angles between the dipole moment and the $\beta$ vector in the py−pym (left) and hy−pym (right) foldamers.

py−pym strand ($0.6 \times 10^2$ au), whereas hy−pym displays a larger and negative response ($-5 \times 10^2$ au). This mainly results from the angle $\theta$ between the dipole moment ($\mu$) and $\beta$ vectors, whose mean value is close to $\pi/2$ (82°) for py−pym, whereas for hy−pym, it amounts to 123° (Figure 4). The $\beta_{\mathrm{EFISHG}}$ distributions of both structures are characterized by very large standard deviations ($\sigma = 3 \times 10^2$ and $10 \times 10^2$ au), demonstrating the crucial role of thermal fluctuations in the EFISHG responses of helical structures. These wide distributions stem from the large fluctuations in the $\theta$ values ($\sigma = 42$ and 70° for py−pym and hy−pym, respectively) as well as the fluctuations in the norm of $\mu$, of similar amplitude to the average value (Figures S15−S16, SI).

In summary, these calculations combining classical samplings with QC evidence the high impact of dynamic fluctuations on the NLO properties in helical strands. In particular, these fluctuations are responsible for relative variations of ~20% in the HRS responses in both structures. Dynamical disorder has an even more important impact on the EFISHG responses, whose variations can reach 2 (py−pym) or 5 (hy−pym) times their mean value. This demonstrates that geometrical fluctuations have necessarily to be taken into account for a reliable description of NLO properties in flexible structures such as helical strands. This work also highlights the relationships between the unit cell nature and helical conformation of foldamers and their second-order NLO responses. In particular, the octupolar symmetry of the HRS depolarization ratios is related to the helix periodicity of three unit cells per turn in both compounds. Following ref 12, this approach can now be used (i) to investigate foldamers bearing donor/acceptor substituents, (ii) to characterize double and quadruple helices,[23] as well as (iii) to study the effects of temperature. In addition, future work will account for solvent−solute interactions, for example, by including explicit solvent molecules in the dynamics and/or by using quantum chemical continuum solvation schemes in the calculation of NLO properties. These further investigations will allow one to propose reliable guidelines for the synthesis of dynamical objects exhibiting large and specific NLO responses.

**Acknowledgment.** The authors thank Prof. J. M. Lehn for suggesting investigating hy−pym strands. E.B. thanks the IAP 6/27 for her postdoctoral grant. B.C. thanks the Fund for Scientific Research (F.R.S.-FNRS) for his research director position. The calculations have been performed on the intensive calculation pole “M3PEC-MESOCENTRE” of the University Bordeaux financed by the Conseil Régional d’Aquitaine and the French Ministry of Research and Technology and on the ISCF installed at the FUNDP, for which the authors gratefully acknowledge the financial support of the F.R.S.-FRFC and the ‘Loterie Nationale’ for the convention No. 2.4617.07, and of the FUNDP.

**Supporting Information Available:** Full geometrical structures optimized at the MMFF94 level of approximation, distributions of the geometrical parameters, and distributions of the HRS and EFISHG quantities. This material is available free of charge via the Internet at http://pubs.acs.org.

## References and Notes

(1) (a) Kanis, D. R.; Ratner, M. A.; Marks, T. J. *Chem. Rev.* **1994**, *94*, 195. (b) Verbiest, T.; Houbrechts, S.; Kauranen, M.; Clays, K.; Persoons, A. *J. Mater. Chem.* **1997**, *7*, 2175. (c) Delaire, J. A.; Nakatani, K. *Chem. Rev.* **2000**, *100*, 1817.

(2) Albert, I. D. L.; Morley, J. O.; Pugh, D. *J. Phys. Chem. A* **1997**, *101*, 1763.

(3) (a) Meyers, F.; Marder, S. R.; Pierce, B. M.; Brédas, J. L. *J. Am. Chem. Soc.* **1994**, *116*, 10703. (b) Kirtman, B.; Champagne, B.; Bishop, D. M. *J. Am. Chem. Soc.* **2000**, *122*, 8007. (c) Xiao, D.; Bulat, F. A.; Yang, W.; Beratan, D. N. *Nano Lett.* **2008**, *8*, 2814.

(4) (a) Moylan, C. R.; Ermer, S.; Lovejoy, S. M.; McComb, I.-H.; Leung, D. S.; Wortmann, R.; Krdmer, P.; Twieg, R. J. *J. Am. Chem. Soc.* **1996**, *118*, 12950. (b) Fischer, P.; Hache, F. *Chirality* **2005**, *17*, 421. (c) Maury, O.; Le Bozec, H. *Acc. Chem. Res.* **2005**, *38*, 691. (d) Bossi, A.; Licandro, E.; Maiorana, S.; Rigamonti, C.; Righetto, S.; Stephenson, G. R.; Spassova, M.; Botek, E.; Champagne, B. *J. Phys. Chem. C* **2008**, *112*, 7900. (e) Keinan, S.; Therien, M. J.; Beratan, D. N.; Yang, W. *J. Phys. Chem. A* **2008**, *112*, 12203.

(5) (a) Xu, H. L.; Li, Z. R.; Wu, D.; Wang, B. Q.; Li, Y.; Gu, F. L.; Aoki, Y. *J. Am. Chem. Soc.* **2007**, *129*, 2967. (b) Boubekeur-Lecaque, L.; Coe, B. J.; Clays, K; Foerier, S.; Verbiest, T.; Asselberghs, I. *J. Am. Chem. Soc.* **2008**, *130*, 3286.

(6) Torrent-Succarat, M.; Sola, M.; Duran, M.; Luis, J. M.; Kirtman, B. *J. Chem. Phys.* **2004**, *120*, 6346.

(7) (a) Kuzyk, M. G. *Phys. Rev. Lett.* **2000**, *85*, 1218. (b) Kuzyk, M. G. *Phys. Rev. Lett.* **2003**, *90*, 039902 (E).

(8) (a) Champagne, B.; Kirtman, B. *Phys. Rev. Lett.* **2005**, *95*, 109401. (b) Kuzyk, M. G. *Phys. Rev. Lett.* **2005**, *95*, 109402.

(9) (a) Schmuck, C. *Angew. Chem., Int. Ed.* **2003**, *42*, 2448. (b) Huc, I. *Eur. J. Org. Chem.* **2004**, 17. (c) Stone, M. J.; Heemstra, J. M.; Moore, J. S. *Acc. Chem. Res.* **2006**, *39*, 11. (d) Petitjean, A.; Cuccia, L. A.; Schmutz, M.; Lehn, J. M. *J. Org. Chem.* **2008**, *73*, 2481.

(10) (a) Ohkita, M.; Lehn, J. M.; Bauum, G.; Fenske, D. *Chem.—Eur. J.* **1999**, *5*, 3471. (b) Schmitt, J. L.; Stadler, A. M.; Kyritsakas, N.; Lehn, J. M. *Helv. Chim. Acta* **2003**, *86*, 1598. (c) Schmitt, J. L.; Lehn, J. M. *Helv. Chim. Acta* **2003**, *86*, 3417.

(11) Halgren, T. A. *J. Comput. Chem.* **1996**, *17*, 490, 520, 553, 587, 616.

(12) Botek, E.; Castet, F.; Champagne, B. *Chem.—Eur. J.* **2006**, *12*, 8687.

(13) Karna, S. P.; Dupuis, M. *J. Comput. Chem.* **1991**, *12*, 487.

(14) Dewar, M. J. S.; Zoebisch, E. G.; Healy, E. F.; Stewart, J. J. P. *J. Am. Chem. Soc.* **1985**, *107*, 3902.

(15) Balakina, M. Y.; Fominykh, O. D.; Rua, F.; Branchadell, V. *Int. J. Quantum Chem.* **2007**, *107*, 2398.

(16) (a) Castet, F.; Champagne, B. *J. Phys. Chem. A* **2001**, *105*, 1366. (b) Botek, E.; Champagne, B. *Appl. Phys. B* **2002**, *74*, 627. (c) Guillaume, M.; Botek, E.; Champagne, B.; Castet, F.; Ducasse, L. *J. Chem. Phys.* **2004**, *121*, 7390. (d) Sanguinet, L.; Pozzo, J. L.; Rodriguez, V.; Adamietz, F.; Castet, F.; Ducasse, L.; Champagne, B. *J. Phys. Chem. B* **2005**, *109*, 11139. (e) Sanguinet, L.; Pozzo, J. L.; Guillaume, M.; Champagne, B.; Castet, F.; Ducasse, L.; Maury, E.; Soulié, J.; Mançois, F.; Adamietz, F.; Rodriguez, V. *J. Phys. Chem. B* **2006**, *110*, 10672. (f) Olejniczak, M.; Pecul, M.; Champagne, B.; Botek, E. *J. Chem. Phys.* **2008**, *128*, 244713.

(17) The Taylor series expansion convention was employed to define $\beta$ with 1 au of $\beta = 3.6213 \times 10^{-42}$ m$^4$ V$^{-1}$ $= 3.20636 \times 10^{-53}$ C$^3$ m$^3$ J$^{-2}$ $= 8.6392 \times 10^{-33}$ esu. See: Shelton, D. P.; Rice, J. E. *Chem. Rev.* **1994**, *94*, 3.

(18) (a) Moylan, C. R.; Ermer, S.; Lovejoy, S. M.; McComb, I.-H.; Leung, D. S.; Wortmann, R.; Krdmer, P.; Twieg, R. J. *J. Am. Chem. Soc.* **1996**, *118*, 12950. (b) Yang, M.; Champagne, B. *J. Phys. Chem. A* **2003**, *107*, 3942. (c) Zrig, S.; Koeckelberghs, G.; Verbiest, T.; Andrioletti, B.; Rose, E.; Persoons, A.; Asselberghs, I.; Clays, K. *J. Org. Chem.* **2007**, *72*, 5855.

(19) Mohamadi, F.; Richards, N. G. J.; Guida, W. C.; Liskamp, R.; Lipton, M.; Caufield, C.; Chang, G.; Hendrickson, T.; Still, W. C. *J. Comput. Chem.* **1990**, *11*, 440.

(20) Stewart, J. J. P. *MOPAC*; Fujitsu: Beaverton, OR, 2002.

(21) (a) Ledoux, I.; Zyss, J.; Siegel, J. S.; Brienne, J.; Lehn, J. M. *Chem. Phys. Lett.* **1990**, *172*, 440. (b) Zyss, J.; Ledoux, I. *Chem. Rev.* **1994**, *94*, 77. (c) Verbiest, T.; Clays, K.; Samyn, C.; Wolff, J.; Reinhoudt, D.; Persoons, A. *J. Am. Chem. Soc.* **1994**, *116*, 9320.

(22) Marder, S. R.; Cheng, L. T.; Tienman, B G.; Friedli, A. C.; Blanchard-Desce, M.; Perry, J. W.; Skindho., J. *Science* **1994**, *263*, 511.

(23) Gan, Q.; Bao, C. Y.; Kauffmann, B.; Grelard, A.; Xiang, J. F.; Liu, S. H.; Huc, I.; Jiang, H. *Angew. Chem., Int. Ed.* **2008**, *47*, 1715.

JP904418R